



Finite-time control for small-scale unmanned helicopter with disturbances

Tao Jiang · Defu Lin · Tao Song

Received: 1 April 2018 / Accepted: 11 March 2019 / Published online: 19 March 2019
© Springer Nature B.V. 2019

Abstract This work aims to develop finite-time stability property for trajectory tracking control system of small-scale unmanned helicopter subjected to uncertainties and external disturbances. The added power integrator method is applied to construct the nominal feedback control part, such that helicopters' closed-loop system possesses highly tracking performance due to finite-time convergence property. In view of the existence of strong couplings, approximate feedback linearization is initially conducted to simplify and decouple helicopters' input–output dynamics. Additionally, to guarantee robustness, the composite active disturbance rejection control idea is employed. These unknown perturbations are estimated using high-order sliding mode disturbance observers and compensated for directly in every virtual control law. Finite-time convergence property of the closed-loop system with disturbances is proven through Lyapunov stability theory. Finally, several comparison simulations illustrate the effectiveness and superiority of our proposed methods.

Keywords Finite-time control · Small-scale unmanned helicopter · Added power integrator method · High-order sliding mode disturbance observer

1 Introduction

Unmanned helicopters have received wide interest in recent decades because of their capabilities, including highly agile maneuvering, vertical taking off and landing, and broad envelope of flight [1,2]. Helicopters have been widely applied into rescue, surveillance, supervision, defense, and other areas. In most of the practical application scenes, helicopters are required to quickly and accurately track a prescribed trajectory. However, controlling unmanned helicopters, especially small-scale ones, is not an easy task due to their complex aerodynamics, strong nonlinearities and dynamic couplings, and significant parameter and model uncertainties [1–4]. To date, designing a high-performance controller for helicopters is still an attractive focus.

In the last decades, many meaningful results for helicopter controls have been proposed. Tradition linear control method, such as PID [1], linear quadratic regulation [5], H_∞ control theory [4–6], and gain-scheduling controllers [7], is based on the model linearized around the trim points that may utilize synthesis techniques. These techniques are convenient for engineering application. However, guaranteeing satisfying performances of the whole system in full enve-

T. Jiang (✉) · D. Lin · T. Song
Beijing Key Laboratory of UAV Autonomous Control,
Beijing Institute of Technology, Beijing 100081, China
e-mail: jiangtao_1992@outlook.com

D. Lin
e-mail: lindf@bit.edu.cn

T. Song
e-mail: 10901034@bit.edu.cn

lope is difficult. Nonlinear control technique, including backstepping [8–12], nonlinear dynamic inversion [13], sliding mode (SM) [14], nonlinear model predictive control [15], and output regulation [16], is applied to conquer this main defect.

Robustness becomes one of the main performance indexes of helicopter given the presence of model uncertainties and external perturbations in its operational environment [1,4]. Traditional robust control strategies, including H_∞ control, SM, and adaptive control, are applied to “inactively” attenuate the effect of disturbance at the cost of sacrificing their nominal performance [17]. Recently, an alternative approach called “active” disturbance reject control (ADRC), which provides a compound controller composed of a nominal feedback control part and a disturbance compensation part, is proposed [17, 18]. The nominal feedback control part guarantees basic stability and closed-loop performance, and the other part provides strong robustness in large-range operation. The compensation part is often designed based on disturbance observer (DO) idea, where the lumped unknown disturbances are estimated by a DO and counteracted online. The disturbances in helicopter dynamics satisfy the mismatched condition, which increases the difficulties in designing a robust controller. Recently, some literatures have applied the ADRC technique to deal with helicopters’ control problem. In [10], the composite backstepping controller combined with nonlinear DO is applied to ensure robust and highly trajectory tracking. [12] adopts extend DO to estimate and compensate for the unknown disturbances, as well as dynamic surface control to guarantee the nominal performance. Nonlinear MPC is combined with DO in [15] to realize highly tracking performance subjected to the perturbations.

To further improve tracking performance, our work aims to develop finite-time (FT) convergence property to helicopter control system. The FT system provides rapid convergent speed around the equilibrium point remarkable disturbance rejection performance, which is an attractive property of a controller design [19, 20]. There are two main theory frameworks to complete finite-time stability analysis, including homogeneous method and Lyapunov-based method [20]. Our work adopts homogeneous domination framework to achieve FT convergence of tracking errors. The added power integrator method [21–23] is applied to design the nominal feedback control part, which ensures nomi-

nal control performance and possesses FT convergence property of the closed-loop system. Additionally, in the recursive design procedure, disturbances are estimated via high-order SM DO (HOSMDO) [24–26] and then feed-forwardly counteracted in virtual control law design of every step. HOSMDO has many excellent properties, such as insensitivity to disturbances and FT convergence. This novel ADRC design guarantees that the tracking error of the closed-loop system converges to zero in FT under disturbances.

The helicopter is a typical multi-input multi-output (MIMO) system, where strong dynamic couplings exist. By approximate feedback linearization, the helicopters’ input–output dynamics enable to be decoupled and simplified [27]. Due to the properties of helicopter model, there exist two subsystems to consist of the decoupled helicopter dynamics, including position system and yaw angle system. Then, the composite FT control strategy is applied to force helicopter’s trajectory to track reference trajectory under internal and external perturbations. The main contributions of our work are summarized as follows:

- (a) FT control strategy based on added power integrator method is applied to deal with trajectory tracking problem of small-scale unmanned helicopters subjected to unknown perturbations. Our proposed FT controller enjoys speed and improved robustness.
- (b) The composite FT control law based on HOSMDO and added power integrator method, which guarantees FT convergence under disturbances, is proposed. Our work develops FT output regulation technique on MIMO system by combining with the approximate input–output linearization technique.
- (c) FT convergence property of tracking errors in the closed-loop system is proven through Lyapunov theory. Comparison simulation results show that the proposed controller features superior performance in trajectory tracking and disturbance rejection.

The configuration of this paper is arranged as follows. Section 2 presents the dynamics of a small-scale helicopter and its linearized model that is obtained by approximated feedback linearization. Section 3 proposes the composite control method, provides the FT stability analysis, and produces practical helicopter control signals. Section 4 discusses the simulations

conducted in this work. Section 5 draws the conclusions.

2 Small-scale helicopter model

2.1 Small-scale helicopter dynamics

The helicopter is considered a six-degree-of-freedom rigid body model with simplified force and moment generation process. Firstly, two reference frames are defined: the earth reference frame (ERF) $\mathbb{I} = \{Oxyz\}$, which is fixed to the earth, and the body reference frame (BRF) $\mathbb{B} = \{O_b x_b y_b z_b\}$ whose origin is located at the helicopter’s center of gravity (c.g.) [3,4]. Figure 1 shows the definition of the two reference frames.

The dynamics of small-scale unmanned helicopter can be described as follows [3,4]:

$$\dot{P} = V, \tag{1}$$

$$\dot{V} = g e_3 + \frac{1}{m} R(\Theta) F, \tag{2}$$

$$\dot{R}(\Theta) = R(\Theta) S(\omega), \tag{3}$$

$$J\dot{\omega} = -\omega \times J\omega + M, \tag{4}$$

where $P = [x \ y \ z]^T$ and $V = [u \ v \ w]^T$ refer to helicopter’s position and velocity vector in the ERF, respectively; m is helicopter’s mass, and g is the gravitational acceleration; $e_3 = [0 \ 0 \ 1]^T$; $S(\cdot)$ is a skew-symmetric matrix that corresponds to the vector (\cdot) [8,9]; and J represents the approximate inertia matrix given as follows:

$$J = \begin{bmatrix} J_{xx} & 0 & -J_{xz} \\ 0 & J_{yy} & 0 \\ -J_{xz} & 0 & J_{zz} \end{bmatrix}. \tag{5}$$

The rotation matrix from BRF to ERF is

$$R(\Theta) = \begin{bmatrix} C_\theta C_\psi & S_\phi S_\theta C_\psi - C_\phi S_\psi & C_\phi S_\theta C_\psi + S_\phi S_\psi \\ C_\theta S_\psi & S_\phi S_\theta S_\psi + C_\phi C_\psi & C_\phi S_\theta S_\psi - S_\phi C_\psi \\ -S_\theta & S_\phi C_\theta & C_\phi C_\theta \end{bmatrix}, \tag{6}$$

where $S_{(\cdot)}$ and $C_{(\cdot)}$ denote $\sin(\cdot)$ and $\cos(\cdot)$, respectively. $\Theta = [\phi \ \theta \ \psi]^T$ are the Euler angles, which include roll, pitch, and yaw angles. $\omega = [p \ q \ r]^T$ denote the angular rates in the BRF. Attitude kinematics are expressed as follows:

$$\dot{\Theta} = \Psi(\Theta) \omega$$

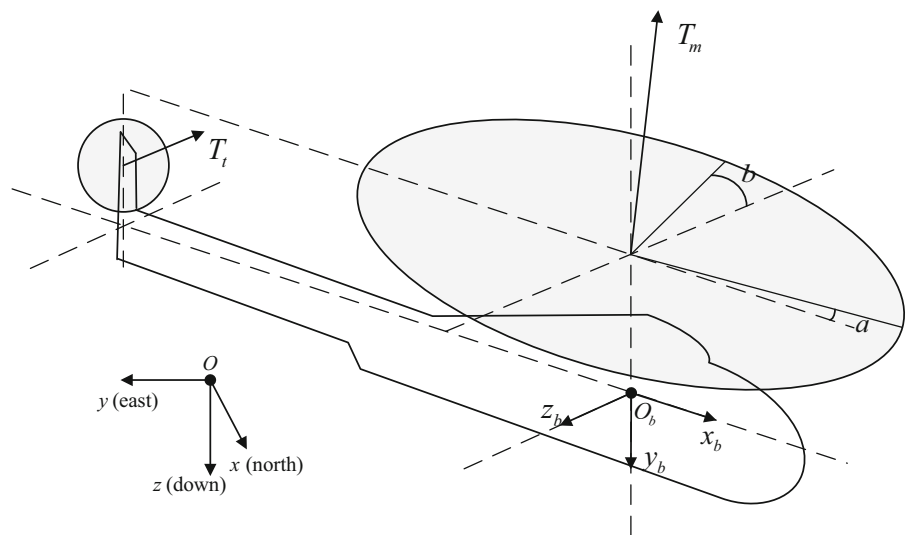
$$\Psi(\Theta) = \begin{bmatrix} 1 & S_\phi C_\theta & C_\phi S_\theta / C_\theta \\ 0 & C_\phi & -S_\phi \\ 0 & S_\phi / C_\theta & C_\phi / C_\theta \end{bmatrix}. \tag{7}$$

In Eqs. (2)–(4), F and M denote the external forces and torque exerted on helicopter’s fuselage in BRF, respectively.

$$F = F_b + F_\Delta, \tag{8}$$

$$M = M_b + M_\Delta,$$

Fig. 1 Simple illustration of a small-scale helicopter model



$$F_b = m \begin{bmatrix} 0 \\ 0 \\ -g + Z_w w + Z_{col} \delta_{col} \end{bmatrix},$$

$$M_b = J (A\omega + Bu_c), \tag{9}$$

where $u_c = [\delta_{col} \delta_{lon} \delta_{lat} \delta_{ped}]^T$ is helicopter’s control input vector, whose elements denote the main rotor’s collective, longitudinal cyclic, lateral cyclic, and the tail rotor’s collective pitch, respectively. F_Δ and M_Δ represent lumped force and torque disturbance in BRP, respectively, that involve external perturbations, parameter variations, and model uncertainties. Constant matrices A and B are expressed as follows [10]:

$$A = \begin{bmatrix} -\tau L_b & -\tau L_a & 0 \\ -\tau M_b & -\tau M_a & 0 \\ 0 & 0 & N_r \end{bmatrix},$$

$$B = \begin{bmatrix} 0 & L_{lon} & L_{lat} & 0 \\ 0 & M_{lon} & M_{lat} & 0 \\ N_{col} & 0 & 0 & N_{ped} \end{bmatrix},$$

where the coefficients $L_b, L_a, M_b, M_a, L_{lon}, L_{lat}, M_{lon}, M_{lat}, N_{col}, N_r, N_{ped}, Z_w$, and Z_{col} depend on the helicopter structure, which can be obtained via system identification technique. Along (8) to (9), helicopter dynamics (2) and (4) can be reexpressed as follows:

$$\dot{V} = ge_3 + R(\Theta) e_3 (-g + Z_w w + Z_{col} \delta_{col}) + \Delta F, \tag{10}$$

$$\dot{\omega} = -J^{-1} (\omega \times J\omega) + (A\omega + Bu_c) + \Delta M \tag{11}$$

where $\Delta F = \frac{1}{m} R(\Theta) F_\Delta$, and $\Delta M = J^{-1} M_\Delta$.

Given the desired smooth trajectory $P_d \triangleq [x_d \ y_d \ z_d]^T$ and yaw angle ψ_d , this work aims to develop control signals $[\delta_{col} \ \delta_{lon} \ \delta_{lat} \ \delta_{ped}]^T$ for a helicopter model with uncertainties and external disturbances, such that its practical trajectory P and yaw angle ψ converge to P_d and ψ_d .

2.2 Approximate feedback linearization

To facilitate controller design and performance analysis, feedback linearization is initially carried out. Traditional exact input–output linearization fails to feedback linearize the whole helicopter system and produces unstable zero dynamics [14,27]. Thus, approximate feedback linearization is developed to simplify and decouple helicopters’ dynamics. This method requires the second-time derivative of the main rotor thrust \ddot{T}_m as

the new input, where $T_m = m (g - Z_w w - Z_{col} \delta_{col})$. The approximated input–output feedback linearization procedure is performed as follows:

First, $e_{p1} = P - P_d$ is obtained. The derivative of e_{p1} from (1) is given as follows:

$$\dot{e}_{p1} = V - \dot{P}_d. \tag{12}$$

Next, let $e_{p2} = V - \dot{P}_d$. Along (10), its derivative is expressed as follows

$$\dot{e}_{p2} = ge_3 - \frac{1}{m} R(\Theta) e_3 T_m + \Delta F - \ddot{P}_d. \tag{13}$$

Selecting $e_{p3} = ge_3 + \frac{1}{m} R(\Theta) T_m - \ddot{P}_d$, the derivative of e_{p3} is derived from (3) as

$$\dot{e}_{p3} = -\frac{1}{m} R(\Theta) S(\omega) e_3 T_m - \frac{1}{m} R(\Theta) e_3 \dot{T}_m - \ddot{P}_d. \tag{14}$$

Define the transition control variables $[M_\phi \ M_\theta \ M_\psi]^T = -J^{-1} (\omega \times J\omega) + (A\omega + Bu_c)$. Let $e_{p4} = -\frac{1}{m} R(\Theta) S(\omega) T_m - \frac{1}{m} R(\Theta) \dot{T}_m - \ddot{P}_d$, along (11), its time derivative is obtained as

$$\dot{e}_{p4} = f_{Pe}(t) + u_P + \Delta M_p, \tag{15}$$

where

$$f_{Pe}(t) = -\frac{1}{m} R(\Theta) S^2(\omega) e_3 T_m - \frac{2}{m} R(\Theta) S(\omega) e_3 \dot{T}_m - P_d^{(4)},$$

$$u_P = -\frac{1}{m} R(\Theta) \begin{bmatrix} T_m M_\theta \\ -T_m M_\phi \\ \ddot{T}_m \end{bmatrix}, \text{ and}$$

$$\Delta M_p = -\frac{1}{m} R(\Theta) \begin{bmatrix} T_m \Delta M(2) \\ -T_m \Delta M(1) \\ 0 \end{bmatrix}.$$

The position error subsystem is approximately feedback-linearized by applying \ddot{T}_m as input. The dynamics of yaw angle errors $e_{\psi 1} = \psi - \psi_d$ is described in Eq. (7) as follows:

$$\dot{e}_{\psi 1} = \frac{S_\phi}{C_\theta} q + \frac{C_\phi}{C_\theta} r - \dot{\psi}_d. \tag{16}$$

Selecting $e_{\psi 2} = \frac{S_\phi}{C_\theta} q + \frac{C_\phi}{C_\theta} r - \dot{\psi}_d$, its derivative yielded along (11) is as follows:

$$\dot{e}_{\psi 2} = f_{\psi e}(t) + u_{\psi} + \Delta M_{\psi}, \tag{17}$$

where

$$f_{\psi e}(t) = \frac{(C_{\phi} \dot{\phi} q + S_{\phi} M_{\theta}) C_{\theta} + (-S_{\phi} \dot{\phi} r + C_{\phi} M_{\psi}) C_{\theta} + S_{\phi} q S_{\theta} \dot{\theta} + C_{\phi} r S_{\theta} \dot{\theta}}{C_{\theta}^2}$$

$$- \ddot{\psi}_d,$$

$$u_{\psi} = \frac{C_{\phi}}{C_{\theta}} M_{\psi}, \text{ and } \Delta M_{\psi} = \frac{S_{\phi}}{C_{\theta}} \Delta M(2) + \frac{C_{\phi}}{C_{\theta}} \Delta M(3).$$

Combining (12)–(17), the complete input–output feedback linearization of helicopter dynamics is given as follows:

$$\begin{aligned} \dot{e}_{P1} &= e_{P2} \\ \dot{e}_{P2} &= e_{P3} + \Delta F \\ \dot{e}_{P3} &= e_{P4} \\ \dot{e}_{P4} &= f_{Pe}(t) + u_P + \Delta M_P \\ \dot{e}_{\psi 1} &= e_{\psi 2} \\ \dot{e}_{\psi 2} &= f_{\psi e}(t) + u_{\psi} + \Delta M_{\psi}. \end{aligned} \tag{18}$$

where u_P and u_{ψ} are regarded as new inputs. The input–output dynamics of helicopters have been decoupled via approximate feedback linearization. Our objective is changed to design the input $[u_P^T \ u_{\psi}^T]^T$ to ensure that tracking errors of the position and yaw angle will converge to zeros.

In addition, the following assumptions are considered to implement the robust controller for helicopter.

Assumption 1 Disturbances ΔF , ΔM_P , and ΔM_{ψ} in (18) satisfy the following condition

$$\begin{aligned} \|\Delta F^{(3)}\| &< \Lambda_F, \quad \|\Delta M_P^{(3)}\| < \Lambda_{M_P}, \\ \|\Delta M_{\psi}^{(3)}\| &< \Lambda_{M_{\psi}}, \end{aligned}$$

where Λ_F , Λ_{M_P} , and $\Lambda_{M_{\psi}}$ are the known constant bound of the third-order time derivative of the disturbances.

Assumption 2 Attitude of the helicopter always lies inside region $|\phi| < \frac{\pi}{2}$ and $|\theta(t)| < \frac{\pi}{2}$.

Remark 1 In (18), ΔF , ΔM_P , and ΔM_{ψ} are lumped disturbances that act on the helicopter model. ΔM_P and ΔM_{ψ} are matched disturbances, whereas ΔF is an unmatched disturbance. The unmatched disturbance ΔF significantly affects tracking precision. Given the existence of unmatched disturbances, various techniques, such as the classic SMC and adaptive control, are restricted.

Remark 2 Assumption 1 ensures the attitude kinematic matrix $\Psi(\Theta)$ in (7) is not singular. This assumption is valid in that the helicopter is considered to operate in hovering or low-velocity flight condition.

2.3 Preliminaries

Preliminary lemmas, which will be used to obtain a FT composite controller later, are illustrated as follows.

Lemma 1 [21]. *Let m be a ratio of positive odd integers. If $0 < m \leq 1$, the following inequalities hold*

$$\begin{aligned} |x^m - y^m| &\leq 2^{1-m} |x - y|^m, \\ (|x| + |y|)^m &\leq |x|^m + |y|^m. \end{aligned}$$

□

Lemma 2 [21]. *Let c_1, c_2 be positive real numbers, and $\gamma(x, y) > 0$ be a real-valued function. Then,*

$$\begin{aligned} |x|^{c_1} |y|^{c_2} &\leq \frac{c_1}{c_1 + c_2} \gamma(x, y) |x|^{c_1+c_2} \\ &\quad + \frac{c_2}{c_1 + c_2} \gamma^{-c_1/c_2}(x, y) |y|^{c_1+c_2}. \end{aligned}$$

□

Lemma 3 [22]. *For $x_i \in R, i = 1, \dots, n$, the inequality $(|x_1| + \dots + |x_n|)^{c_p} \leq |x_1|^{c_p} + \dots + |x_n|^{c_p}$ holds where c_p is a real number that satisfies $0 < c_p \leq 1$.*

□

Theorem 1 [20]. *Considering $\dot{x} = f(x), x \in \mathcal{N}$. Suppose a continuous function $V(x)$ exists such that the following conditions hold:*

- (a) $V(x)$ is positive definite.
- (b) Real number $c_v > 0$ and $\alpha \in (0, 1)$ exist such that

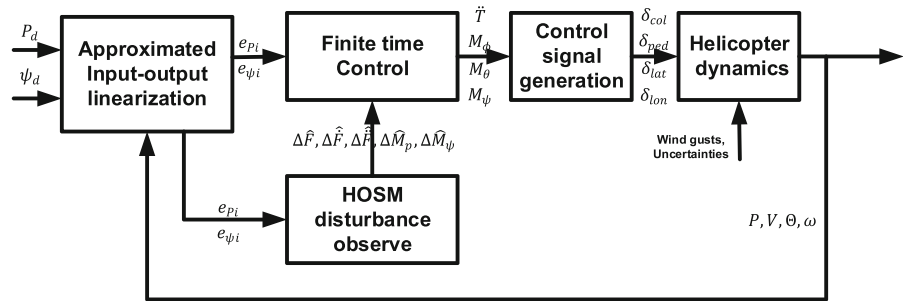
$$V(x) + c_v (V(x))^{\alpha} < 0, \quad x \in \mathcal{N} \setminus \{0\}.$$

Then, the origin is a FT stable equilibrium. □

3 Helicopter controller design

This section expresses the design of the proposed helicopter’s FT control. First, HOSMDO is applied to estimate lumped force and moment disturbances. Second, composite control strategy based on DO and FT control is proposed. At the same time, the FT stability analysis is provided in detail. Finally, the practical control signals for helicopter are produced directly. Figure 2 depicts the control system structure.

Fig. 2 FT controller structure diagram



3.1 HOSMDO

Considering the dynamic system

$$\dot{x}_j = f_j(t) + d_j(t), \tag{19}$$

where $x_j \in \mathbb{R}^n$ denotes the system state; $f_j(t)$ is the known nonlinear smooth function; $d_j(t) \in \mathbb{R}^n$ are unknown bounded perturbation terms due to model uncertainty and external disturbances. Assume that the disturbance $d_j(t)$ owns the bounded r th-order time derivative, i.e., $\|d_j^{(r)}(t)\| < L_j$. To obtain the estimation of disturbance and its high-order derivatives, a HOSMDO of $d_j(t)$ is designed as follows [24].

$$\begin{aligned} \dot{z}_{0,j} &= f_j(t) + v_0, \quad v_0 = z_1 \\ &\quad -\lambda_0 L_j^{\frac{1}{r+1}} |z_{0,j} - x_j|^{\frac{r}{r+1}} \text{sign}(z_{0,j} - x_j) \\ \dot{z}_{1,j} &= v_{1,j}, \quad v_{1,j} = z_{2,j} \\ &\quad -\lambda_1 L_j^{\frac{1}{r}} |z_{1,j} - v_{0,j}|^{\frac{r-1}{r}} \text{sign}(z_{1,j} - v_{0,j}) \\ &\vdots \\ \dot{z}_{r-1,j} &= v_{r-1,j}, \quad v_{r-1,j} = z_{r,j} \\ &\quad -\lambda_{r-1} L_j^{\frac{1}{2}} |z_{r-1,j} - v_{r-2,j}|^{\frac{1}{2}} \\ &\quad \text{sign}(z_{r-1,j} - v_{r-2,j}) \\ \dot{z}_{r,j} &= v_{r,j}, \quad v_{r,j} = -\lambda_r L_j \text{sign}(z_{r,j} - v_{r-1,j}) \end{aligned} \tag{20}$$

where $\lambda_0, \lambda_1, \dots, \lambda_{r-1}, \lambda_r$ are the observer parameters. $z_{0,j}, z_{1,j}, \dots, z_{r-1,j}, z_{r,j}, j = 1, 2, 3$, are the estimates of $x_j, d_j, \dots, d_j^{(r-2)}, d_j^{(r-1)}$.

Considering that the estimated variables are vector, the multivariable calculation form is adopted, such as $\text{sign}(X) = \left[\frac{x_1}{|x_1|}, \dots, \frac{x_n}{|x_n|} \right]$, where $X = [x_1, \dots, x_n]$, and $|X|^l = [|x_1|^l, \dots, |x_n|^l]$. Due to no existence of coupling in (19), the system's properties and analysis process is the same as the scalar system.

Followed from (19)–(20), the observer error dynamics are then governed by:

$$\begin{aligned} \dot{\sigma}_{0,j} &= -\lambda_0 L_j^{\frac{1}{r+1}} |\sigma_{0,j}|^{\frac{r}{r+1}} \text{sign}(\sigma_{0,j}) + \sigma_{1,j} \\ \dot{\sigma}_{i,j} &= -\lambda_1 L_j^{\frac{1}{r}} |\sigma_{i,j} - \dot{\sigma}_{i-1,j}|^{\frac{r-1}{r}} \text{sign}(\sigma_{i,j} - \dot{\sigma}_{i-1,j}) \\ &\quad + \sigma_{i+1,j} \\ &\vdots \\ \dot{\sigma}_{r,j} &= -\lambda_r L_j \text{sign}(\sigma_{r,j} - \dot{\sigma}_{r-1,j}) \end{aligned} \tag{21}$$

where the observer errors are denoted as $\sigma_{0,j} = z_{0,j} - x_j$, $\sigma_{i,j} = z_{i,j} - d_j^{(i-1)}$, and $\sigma_{r,j} = z_{r,j} - d_j^{(r-1)}$. The FT convergence of estimation error is given by the following theory.

Theorem 2 [24]. *The parameters in (20) are properly selected, and the following equalities are true after a FT transient process*

$$\begin{aligned} \sigma_{0,j} = \dots = \sigma_{r,j} &= 0, \quad \text{when } t > t_j \\ \text{i.e.,} \\ z_{0,j} = x_j, \quad z_{1,j} = v_{0,j} = d_j, \dots, \quad z_{r,j} &= d_j^{(r-1)}, \\ \text{when } t > t_j. \end{aligned} \tag{22}$$

□

Remark 3 The selection of L_j is a trade-off process. Large parameters L_j mean fast convergence rate of HOSMDO. However, the parameters L_j with large values cannot be selected to avoid excessive transient peaking in system responses.

Given ΔF in Eq. (18), applying HOSMDO its value and high derivatives can be estimated by explicitly defining $x_1 = e_{p2}, f_1(t) = e_{p3}$, and $d_1(t) = \Delta F$. After FT t_1 , we have $z_{1,1} = \Delta F, z_{2,1} = \Delta \dot{F}, z_{3,1} = \Delta \ddot{F}$. Similarly, the disturbances $\Delta M_p, \Delta M_\psi$ can be observed by selecting $x_2 = e_{p4}, f_2(t) = f_{pe}(t), d_2(t) = \Delta M_p$, and $x_3 = e_{\psi 2}, f_3(t) = f_{\psi e}(t),$

$$d_3(t) = \Delta M_\psi. \text{ After time } \max\{t_2, t_3\}, z_{1,2} = \Delta M_p, z_{2,2} = \Delta \dot{M}_p, z_{3,2} = \Delta \ddot{M}_p, \text{ and } z_{1,3} = \Delta M_\psi, z_{2,3} = \Delta \dot{M}_\psi, z_{3,3} = \Delta \ddot{M}_\psi.$$

3.2 FT controller design

Consider the properties of FT convergence of HOS-MDO. After time $t_{\max} = \max\{t_1, t_2, t_3\}$, the dynamics in (18) can be rewritten as

$$\begin{aligned} \dot{e}_{p1} &= e_{p2} \\ \dot{e}_{p2} &= e_{p3} + z_{1,1} \\ \dot{e}_{p3} &= e_{p4} \\ \dot{e}_{p4} &= f_{pe}(t) + u_p + z_{1,2} \\ \dot{e}_{\psi 1} &= e_{\psi 2} \\ \dot{e}_{\psi 2} &= f_{\psi e}(t) + u_\psi + z_{1,3} \end{aligned} \tag{23}$$

In this subsection, the compound control strategy is proposed based on (23) to simplify the control design. The position error loop in (23) is the vector form with three components, namely, $e_{pi} = [e_{pi,1} \ e_{pi,2} \ e_{pi,3}]^T$, $z_{1,j} = [z_{1,j,1} \ z_{1,j,2} \ z_{1,j,3}]^T$, $u_p = [u_{p,1} \ u_{p,2} \ u_{p,3}]^T$, and $i = 1, \dots, 4, j = 1, 2, 3$. At the same time, mismatched disturbance exists in the position loop.

Position loop controller design

Step 1 Considering dynamics (23), let a Lyapunov function be

$$V_1 = \sum_{i=1}^3 \int_0^{e_{p1,i}} (s^{1/r_1})^{2-r_2} ds, \tag{24}$$

where $r_1 = 1, r_i = r_{i-1} + \tau, -1/5 < \tau < 0$. V_1 is positive by selecting the parameter τ as a ratio of even and odd integers.

The derivative of (24) along (23) is given as

$$\dot{V}_1 \leq \sum_{i=1}^3 e_{p1,i}^{(2-r_2)/r_1} \cdot e_{p2,i}. \tag{25}$$

Applying the concept of backstepping, the virtual control law is arranged as

$$e_{p2,i}^* = -\beta_1 e_{p1,i}^{r_2/r_1}, \quad i = 1, 2, 3, \tag{26}$$

where $\beta_1 > 3c + \tilde{\beta}_1 > 0, \tilde{\beta}_1 > 0$ are the designed controller constant. Introducing (26) into (25)

$$\begin{aligned} \dot{V}_1 &\leq \sum_{i=1}^3 \left(-(\beta_1 + 3c) e_{p1,i}^{2/r_1} + e_{p1,i}^{(2-r_2)/r_1} \right. \\ &\quad \left. \cdot (e_{p2,i} - e_{p2,i}^*) \right). \end{aligned} \tag{27}$$

Step 2 In this step, the Lyapunov function is selected as

$$V_2 = V_1 + \sum_{i=1}^3 \left(\int_{e_{p2,i}^*}^{e_{p2,i}} \left(s^{1/2} - (e_{p2,i}^*)^{1/2} \right)^{2-r_3} ds \right). \tag{28}$$

Computing its time derivative along (23), (27), and (28) yields

$$\begin{aligned} \dot{V}_2 &\leq -\sum_{i=1}^3 \left(-\beta_1 e_{p1,i}^{r_2/r_1} + e_{p1,i}^{r_2/r_1} (e_{p2,i} - e_{p2,i}^*) \right) \\ &\quad + \sum_{i=1}^3 \left((\xi_{2,i})^{2-r_3} (e_{p3,i} + z_{1,1,i}) + (2-r_3) \right. \\ &\quad \left. \times \int_{e_{p2,i}^*}^{e_{p2,i}} \left(s^{1/2} - (e_{p2,i}^*)^{1/2} \right)^{1-r_3} ds \frac{\partial (e_{p2,i}^*)^{1/2}}{\partial e_{p1,i}} \dot{e}_{p1,i} \right) \end{aligned} \tag{29}$$

where $\xi_{2,i} = (e_{p2,i})^{1/2} - (e_{p2,i}^*)^{1/2}, i = 1, 2, 3$. The following relationships are established by applying Lemmas 1–2 directly.

$$\begin{aligned} e_{p1,i}^{r_2/r_1} \cdot (e_{p2,i} - e_{p2,i}^*) &\leq 2^{1-r_2} |e_{p1,i}|^{r_2/r_1} |\xi_{2,i}|^{r_2} \\ &\leq \frac{c}{2} |e_{p1,i}|^2 + C_{11} |\xi_{2,i}|^2 \\ (2-r_3) \int_{e_{p2,i}^*}^{e_{p2,i}} \left(s^{1/2} - (e_{p2,i}^*)^{1/2} \right)^{1-r_3} ds \frac{\partial (e_{p2,i}^*)^{1/2}}{\partial e_{p1,i}} \dot{e}_{p1,i} \\ &\leq (2-r_3) (\xi_{2,i})^{1-r_3} (e_{p2,i} - e_{p2,i}^*) \frac{\partial \left(-\beta_1 e_{p1,i}^{r_2/r_1} \right)^{1/2}}{\partial e_{p1,i}} e_{p2,i} \\ &\leq (-\beta_1)^{1/r_2} (2-r_3) 2^{1-r_2} (\xi_{2,i})^{1-r_3} |\xi_{2,i}|^{r_2} \\ &\quad \times \left(|e_{p2,i} - e_{p2,i}^*| + |\beta_1 e_{p1,i}^{r_2/r_1}| \right) \\ &\leq (-\beta_1)^{1/r_2} (2-r_3) 2^{1-r_2} |\xi_{2,i}|^{1-\tau} \\ &\quad \times \left(2^{1-r_2} |\xi_{2,i}|^{r_2} + |\beta_1 e_{p1,i}^{r_2/r_1}| \right) \\ &\leq \frac{c}{2} |e_{p1,i}|^2 + C_{12} |\xi_{2,i}|^2 \end{aligned}$$

where the constants $C_{11} > 0$ and $C_{12} > 0$. Substituting the following results into (29), we arrive at

$$\begin{aligned} \dot{V}_2 \leq & \sum_{i=1}^3 \left(-(\beta_1 - c) e_{P1,i}^2 + (C_{11} + C_{12}) |\xi_{2,i}|^2 \right. \\ & \left. + (\xi_{2,i})^{2-r_3} (e_{P3,i} + z_{1,1,i}) \right). \end{aligned} \tag{30}$$

The virtual controller is designed as

$$e_{P3,i}^* = -\beta_2 (\xi_{2,i})^{r_3} - z_{1,1,i}, \quad i = 1, 2, 3, \tag{31}$$

where $\beta_2 > C_{11} + C_{12} + \tilde{\beta}_2 + 2c$, $\tilde{\beta}_2 > 0$ are selected. Combining (30) and (31) renders

$$\begin{aligned} \dot{V}_2 \leq & \sum_{i=1}^3 \left(-(\tilde{\beta}_1 + 2c) e_{P1,i}^2 - (\tilde{\beta}_2 + 2c) |\xi_{2,i}|^2 \right. \\ & \left. + (\xi_{2,i})^{2-r_3} (e_{P3,i} - e_{P3,i}^*) \right). \end{aligned} \tag{32}$$

Step 3 Lyapunov function is defined as

$$V_3 = V_2 + \sum_{i=1}^3 \left(\int_{\bar{e}_{P3,i}^*}^{\bar{e}_{P3,i}} \left(s^{\frac{1}{r_3}} - (\bar{e}_{P3,i}^*)^{\frac{1}{r_3}} \right)^{2-r_4} ds \right), \tag{33}$$

where $\bar{e}_{P3,i} = e_{P3,i} + z_{1,1,i} = -\beta_2 (\xi_{2,i})^{r_3}$, $\bar{e}_{P3,i} = e_{P3,i} + z_{1,1,i}$, and $i = 1, 2, 3$. The derivative is obtained along (23) and (32)

$$\begin{aligned} \dot{V}_3 \leq & \sum_{i=1}^3 \left(-(\beta_1 - c) e_{P1,i}^2 - \beta_2 |\xi_{2,i}|^2 \right. \\ & \left. + (\xi_{2,i})^{2-r_3} (e_{P3,i} - e_{P3,i}^*) \right) \\ & + \sum_{i=1}^3 \left(\begin{aligned} & (\xi_{3,i})^{2-r_4} (e_{P4,i} + z_{2,1,i}) \\ & + (2 - r_4) \int_{\bar{e}_{P3,i}^*}^{\bar{e}_{P3,i}} \left(s^{\frac{1}{r_3}} - (\bar{e}_{P3,i}^*)^{\frac{1}{r_3}} \right)^{1-r_4} ds \left(\frac{\partial(\bar{e}_{P3,i}^*)^{\frac{1}{r_3}}}{\partial e_{P1,i}} \dot{e}_{P1,i} \right. \\ & \left. + \frac{\partial(\bar{e}_{P3,i}^*)^{\frac{1}{r_3}}}{\partial e_{P2,i}} \dot{e}_{P2,i} \right) \end{aligned} \right) \end{aligned} \tag{34}$$

where $\xi_{3,i} = (\bar{e}_{P3,i})^{\frac{1}{r_3}} - (\bar{e}_{P3,i}^*)^{\frac{1}{r_3}}$. To construct a FT stabilizer, the inequalities are introduced as follows

$$\begin{aligned} (\xi_{2,i})^{2-r_3} (e_{P3,i} - e_{P3,i}^*) & \leq 2^{1-r_3} |\xi_{2,i}|^{2-r_3} |\xi_{3,i}|^{r_3} \\ & \leq \frac{c}{2} |\xi_{2,i}|^2 + C_{21} |\xi_{3,i}|^2 \\ (2 - r_4) \int_{\bar{e}_{P3,i}^*}^{\bar{e}_{P3,i}} \left(s^{\frac{1}{r_3}} - (\bar{e}_{P3,i}^*)^{\frac{1}{r_3}} \right)^{1-r_4} ds \\ & \times \left(\frac{\partial(\bar{e}_{P3,i}^*)^{\frac{1}{r_3}}}{\partial e_{P1,i}} \dot{e}_{P1,i} + \frac{\partial(\bar{e}_{P3,i}^*)^{\frac{1}{r_3}}}{\partial e_{P2,i}} \dot{e}_{P2,i} \right) \end{aligned}$$

$$\begin{aligned} & \leq (2 - r_4) 2^{1-r_3} |\xi_{3,i}|^{1-r_4} |\xi_{3,i}|^{r_3} \\ & \left(\frac{\partial(\bar{e}_{P3,i}^*)^{\frac{1}{r_3}}}{\partial e_{P1,i}} \dot{e}_{P1,i} + \frac{\partial(\bar{e}_{P3,i}^*)^{\frac{1}{r_3}}}{\partial e_{P2,i}} \dot{e}_{P2,i} \right) \end{aligned}$$

where

$$\begin{aligned} \frac{\partial(\bar{e}_{P3,i}^*)^{\frac{1}{r_3}}}{\partial e_{P1,i}} \dot{e}_{P1,i} & \leq \frac{\partial(\bar{e}_{P3,i}^*)^{\frac{1}{r_3}}}{\partial e_{P1,i}} \\ & \times \left((2^{1-r_2} |\xi_{2,i}|^{r_2} + |\beta_1 e_{P1,i}^{r_2}|) \right) \\ & \leq \tilde{c}_{3,1} \frac{\partial(e_{P1,i})^{\frac{1}{r_1}}}{\partial e_{P1,i}} \left(2^{1-r_2} |\xi_{2,i}|^{r_2} + |\beta_1 e_{P1,i}^{r_2}| \right) \\ & = \tilde{c}_{3,1} \left(2^{1-r_2} |\xi_{2,i}|^{r_2} + |\beta_1 e_{P1,i}^{r_2}| \right) \\ \frac{\partial(\bar{e}_{P3,i}^*)^{\frac{1}{r_3}}}{\partial e_{P2,i}} \dot{e}_{P2,i} & \leq \frac{\partial(\bar{e}_{P3,i}^*)^{\frac{1}{r_3}}}{\partial e_{P2,i}} \\ & \times \left(2^{1-r_3} |\xi_{3,i}|^{r_3} + (C_{11} + C_{12} + \beta_2) |\xi_{2,i}|^{r_3} \right) \\ & \leq \frac{\tilde{c}_{3,2}}{r_2} \left(|\xi_{2,i}| + (e_{P2,i}^*)^{\frac{1}{r_2}} \right)^{1-r_2} \\ & \times \left(2^{1-r_3} |\xi_{3,i}|^{r_3} + \beta_2 |\xi_{2,i}|^{r_3} \right) \end{aligned}$$

Combining the aforementioned analysis by applying Lemma 2 yields

$$\begin{aligned} (2 - r_4) \int_{\bar{e}_{P3,i}^*}^{\bar{e}_{P3,i}} \left(s^{\frac{1}{r_3}} - (\bar{e}_{P3,i}^*)^{\frac{1}{r_3}} \right)^{1-r_4} ds \\ \times \left(\frac{\partial(\bar{e}_{P3,i}^*)^{\frac{1}{r_3}}}{\partial e_{P1,i}} \dot{e}_{P1,i} + \frac{\partial(\bar{e}_{P3,i}^*)^{\frac{1}{r_3}}}{\partial e_{P2,i}} \dot{e}_{P2,i} \right) \\ \leq c |e_{P1,i}|^2 + \frac{c}{2} |\xi_{2,i}|^2 + C_{22} |\xi_{3,i}|^2 \end{aligned}$$

Then, substituting the aforementioned results into (34) renders

$$\begin{aligned} \dot{V}_3 \leq & \sum_{i=1}^3 \left(-(\beta_1 - 2c) e_{P1,i}^2 - (\beta_2 - c) |\xi_{2,i}|^2 \right. \\ & + (\xi_{3,i})^{2-r_4} (e_{P4,i} + z_{2,1,i}) \\ & \left. + C_{21} |\xi_{3,i}|^2 + C_{22} |\xi_{3,i}|^2 \right). \end{aligned} \tag{35}$$

The virtual control is given as

$$e_{P4,i}^* = -\beta_3 (\xi_{3,i})^{r_4} - z_{2,1,i}, \quad i = 1, 2, 3, \tag{36}$$

where $\beta_3 > C_{21} + C_{22} + \tilde{\beta}_3 + c$, $\tilde{\beta}_3 > 0$. Thus, the corresponding Lyapunov function satisfies

$$\begin{aligned} \dot{V}_3 \leq & \sum_{i=1}^3 \left(-(\tilde{\beta}_1 + c) e_{P1,i}^2 - (\tilde{\beta}_2 + c) |\xi_{2,i}|^2 \right. \\ & \left. - (\tilde{\beta}_3 + c) |\xi_{3,i}|^2 + (\xi_{3,i})^{2-r_4} (e_{P4,i} - e_{P4,i}^*) \right) \end{aligned} \tag{37}$$

Step 4 Lyapunov function is selected as

$$V_4 = V_3 + \sum_{i=1}^3 \left(\int_{\bar{e}_{P4,i}^*}^{\bar{e}_{P4,i}} \left(s^{\frac{1}{r_4}} - (\bar{e}_{P4,i}^*)^{\frac{1}{r_4}} \right)^{2-r_5} ds \right), \tag{38}$$

where $\bar{e}_{P4,i}^* = e_{P4,i}^* + z_{2,1,i} = -\beta_3 (\xi_{3,i})^{r_4}$, and $\bar{e}_{P4,i} = e_{P4,i} + z_{2,1,i}$. Similarly, computing the time derivative of (38) yields

$$\begin{aligned} \dot{V}_4 \leq & \sum_{i=1}^3 \left(-(\beta_1 - 2c) e_{P1,i}^2 - (\beta_2 - c) |\xi_{2,i}|^2 \right. \\ & - \beta_3 |\xi_{3,i}|^2 + |\xi_{3,i}|^{2-r_4} (e_{P4,i} - e_{P4,i}^*) \\ & + \sum_{i=1}^3 \left(|\xi_{4,i}|^{2-r_5} (f_{Pe,i}(t) + u_{P,i} + z_{1,2,i} \right. \\ & \left. + z_{3,1,i}) + (2 - r_5) \zeta_4 \right. \\ & \left. \times \int_{\bar{e}_{P4,i}^*}^{\bar{e}_{P4,i}} \left(s^{\frac{1}{r_4}} - (\bar{e}_{P4,i}^*)^{\frac{1}{r_4}} \right)^{1-r_5} ds \right) \\ \leq & \sum_{i=1}^3 \left(-(\beta_1 - 3) e_{P1,i}^2 - (\beta_2 - 2) |\xi_{2,i}|^2 \right. \\ & - (\beta_3 - 1) |\xi_{3,i}|^2 + |\xi_{4,i}|^{2-r_5} (f_{Pe,i}(t) + u_{P,i} \\ & \left. + z_{1,2,i} + z_{3,1,i}) + C_{31} |\xi_{4,i}|^2 + C_{32} |\xi_{4,i}|^2 \right) \end{aligned} \tag{39}$$

$$\begin{aligned} \text{where } \zeta_4 = & \frac{\partial (\bar{e}_{P4,i}^*)^{\frac{1}{r_4}}}{\partial e_{P1,i}} \dot{e}_{P1,i} + \frac{\partial (\bar{e}_{P4,i}^*)^{\frac{1}{r_4}}}{\partial e_{P2,i}} \dot{e}_{P2,i} + \frac{\partial (\bar{e}_{P4,i}^*)^{\frac{1}{r_4}}}{\partial e_{P3,i}} \\ & \dot{e}_{P3,i}, \xi_{4,i} = (\bar{e}_{P4,i})^{\frac{1}{r_4}} - (\bar{e}_{P4,i}^*)^{\frac{1}{r_4}}. \end{aligned}$$

The position controller is designed as

$$\begin{aligned} u_{P,i} = & -\beta_4 (\xi_{4,i})^{r_5} - f_{Pe,i}(t) - z_{1,2,i} - z_{3,1,i}, \\ & i = 1, 2, 3, \end{aligned} \tag{40}$$

where $\beta_4 > C_{31} + C_{32} + \tilde{\beta}_4 > 0$. Substituting (40) into (39) introduces

$$\begin{aligned} \dot{V}_4 \leq & \sum_{i=1}^3 \left(-\tilde{\beta}_1 e_{P1,i}^2 - \tilde{\beta}_2 |\xi_{2,i}|^2 \right. \\ & \left. - \tilde{\beta}_3 |\xi_{3,i}|^2 - \tilde{\beta}_4 |\xi_{4,i}|^2 \right). \end{aligned} \tag{41}$$

Yaw angle loop controller design

Step 1 Define a Lyapunov function

$$V_{1\psi} = \int_0^{e_{\psi 1}} \left(s^{1/r_1} \right)^{2-r_2} ds. \tag{42}$$

Considering (23), the first time derivative is given as

$$\dot{V}_{1\psi} = e_{\psi 1}^{(2-r_2)/r_1} \cdot e_{\psi 2}. \tag{43}$$

Design the virtual control as

$$e_{\psi 2}^* = -\beta_{1\psi} e_{\psi 1}^{r_2/r_1}, \tag{44}$$

thus

$$\dot{V}_{1\psi} = -\beta_{1\psi} e_{\psi 1}^2 + e_{\psi 1}^{2-r_2} \cdot (e_{\psi 2} - e_{\psi 2}^*), \tag{45}$$

where the constant $\beta_{1\psi} > c_{\psi} + \tilde{\beta}_{1\psi} > 0$, $\tilde{\beta}_{1\psi} > 0$.

Step 2 The Lyapunov function is selected as

$$V_{2\psi} = V_{1\psi} + \int_{e_{\psi 2}^*}^{e_{\psi 2}} \left(s^{\frac{1}{r_2}} - (e_{\psi 2}^*)^{\frac{1}{r_2}} \right)^{2-r_3} ds. \tag{46}$$

Calculating its derivative yields

$$\begin{aligned} \dot{V}_{2\psi} = & -\beta_{1\psi} e_{\psi 1}^2 + e_{\psi 1}^{2-r_2} \cdot (e_{\psi 2} - e_{\psi 2}^*) \\ & + (\xi_{2\psi})^{2-r_3} (f_{\psi e}(t) + u_{\psi} + z_{1,3}) \\ & + (2 - r_3) \int_{e_{\psi 2}^*}^{e_{\psi 2}} \left(s^{\frac{1}{r_2}} - (e_{\psi 2}^*)^{\frac{1}{r_2}} \right)^{1-r_3} ds \frac{\partial (e_{\psi 2}^*)^{\frac{1}{r_2}}}{\partial e_{\psi 1}} \dot{e}_{\psi 1} \end{aligned}$$

$$\begin{aligned} &\leq -(\beta_{1\psi} - 1)e_{\psi 1}^2 + (C_{1\psi} + C_{2\psi})|\xi_{2\psi}|^2 \\ &\quad + (\xi_{2\psi})^{2-r_3}(f_{\psi e}(t) + u_{\psi} + z_{1,3}) \end{aligned} \tag{47}$$

where $\xi_{2\psi} = (e_{\psi 2})^{\frac{1}{r_2}} - (e_{\psi 2}^*)^{\frac{1}{r_2}}$. Selecting

$$u_{\psi} = -\beta_{2\psi}(\xi_{2\psi})^{r_3} - f_{\psi e}(t) - z_{1,3}, \tag{48}$$

where the control constant $\beta_{2\psi} > C_{1\psi} + C_{2\psi} + \tilde{\beta}_{2\psi} > 0$, $\tilde{\beta}_{2\psi} > 0$ yields

$$\dot{V}_{2\psi} \leq -\tilde{\beta}_{1\psi}e_{\psi 1}^2 - \tilde{\beta}_{2\psi}|\xi_{2\psi}|^2. \tag{49}$$

3.3 Proof of FT stability

Based on the FT Lyapunov theory, FT stability of the whole system is proven. The detailed proof is given in appendix.

Theorem 3 Consider that the simplified helicopter dynamic system satisfies Assumptions 1 and 2. Proposed controller (40) and (48) can guarantee that the closed-loop system is FT stable. □

Remark 4 In the position controller u_P and yaw angle controller u_{ψ} , the control design parameters include τ , $\beta_1, \beta_2, \beta_3, \beta_4, \beta_{1\psi}$, and $\beta_{2\psi}$. Deciding the value of these parameter is a trade-off process. Larger values mean faster closed-loop system state convergence. However, large values cause excessive inputs and overshoot. For our problem, the principle for selecting parameters depends on the dynamic characteristic of small-scale helicopters.

3.4 Practical helicopter control signal

The practical control signals for helicopter can be calculated from u_P in (40) and u_{ψ} in (48). According to their definitions, one has

$$\begin{bmatrix} M_{\phi} \\ M_{\theta} \\ \ddot{T}_m \end{bmatrix} = -m \cdot \begin{bmatrix} 0 & T_m & 0 \\ -T_m & 0 & 0 \\ 0 & 0 & 1 \end{bmatrix} \cdot R^{-1}(\Theta) \cdot u_P, \tag{50}$$

$$M_{\psi} = \frac{C_{\theta}}{C_{\phi}}u_{\psi}. \tag{51}$$

Following that, the control commands $[\delta_{col} \ \delta_{lon} \ \delta_{lat} \ \delta_{ped}]^T$ can be obtained according to the definition of $[M_{\phi} \ M_{\theta} \ M_{\psi}]^T$ and $T_M = \int_0^t \ddot{T}_m dt$.

$$\delta_{col} = -\left(\frac{T_m}{m} - g + Z_w w\right) / Z_{col}, \tag{52}$$

$$\begin{bmatrix} \delta_{lon} \\ \delta_{lat} \\ \delta_{ped} \end{bmatrix} = \begin{bmatrix} M_{\phi} \\ M_{\theta} \\ M_{\psi} \end{bmatrix} + J^{-1}(\omega \times J\omega) - A\omega - B(1)\delta_{col}, \tag{53}$$

where $B(1)$ is the first column of matrix B .

The following result is given directly by applying Theorem 3.

Theorem 4 Consider helicopter dynamic models (1)–(4) under Assumptions 1 and 2. If the controller is designed as (52)–(53), then tracking errors of the position and yaw angle FT converge to zero with disturbances. □

4 Simulation analysis

Numerical simulations are shown to demonstrate the effectiveness of our proposed FT controller. Table 1

Table 1 Parameters of the helicopter

Symbol	Description	Value
m	Mass of unmanned helicopter	8.2 kg
g	Acceleration of gravity	9.8 m/s ²
J	The moment of inertia of helicopter	diag(0.18 0.34 0.28) kg m ²
Z_w	Linkage gain ratio of T_m to w	-0.7615 s ⁻¹
Z_{col}	Linkage gain ratio of T_m to δ_{col}	-131.4125m/(rad s ²)
A	Coefficient matrix of Ω in (9)	diag(-48.1757 - 25.5048 - 0.9808) s ⁻¹
B	Coefficient matrix of u in (9)	$\begin{bmatrix} 0 & 0 & 1689.5 & 0 \\ 0 & 894.5 & 0 & 0 \\ -0.3705 & 0 & 0 & 135.8 \end{bmatrix}$ s ⁻²

summarizes the corresponding helicopter model parameters [10, 28].

Following [10], the lumped disturbances in (10)–(11) are introduced in the simulation. These disturbances include model uncertainties and external disturbances.

$$\begin{bmatrix} \Delta F \\ \Delta M \end{bmatrix} = \Delta \cdot \begin{bmatrix} V \\ \Theta \\ \omega \end{bmatrix} + B_{wind}d_{wind}, \tag{54}$$

where constant matrix $\Delta \in R^{6 \times 9}$ represents model uncertainty, and B_{wind} denotes the transformation matrix from airspeed to force and moment. All elements of Δ are pseudorandomly generated within the open interval $(-0.5, 0.5)$. Matrices Δ and B_{wind} are given as follows:

$$\Delta = \begin{bmatrix} -0.239 & 0.164 & -0.055 & 0.456 & 0.013 & -0.362 & -0.096 & 0.071 & -0.185 \\ 0.203 & 0.351 & 0.419 & 0.351 & -0.135 & 0.342 & 0.491 & -0.359 & -0.387 \\ 0.035 & 0.165 & 0.232 & 0.265 & -0.384 & 0.254 & -0.044 & 0.357 & 0.031 \\ 0.311 & 0.045 & 0.369 & -0.250 & -0.303 & -0.368 & -0.352 & 0.012 & -0.011 \\ -0.055 & -0.465 & 0.062 & 0.290 & 0.048 & -0.451 & 0.426 & -0.454 & 0.209 \\ 0.267 & -0.409 & -0.088 & -0.482 & 0.057 & 0.459 & 0.138 & -0.028 & 0.343 \end{bmatrix}$$

$$B_{wind} = m \cdot \begin{bmatrix} -0.0505 & 0 \\ 0 & -0.151 \\ 0 & 0 \\ -0.144 & 0.143 \\ -0.0561 & -0.0585 \\ 0 & 0.0301 \end{bmatrix}$$

Wind disturbance d_w is assumed to possess wind components along $[x_b \ y_b]$ in BRF. This variable is composed of constant and random components, i.e., $d_w = d_c + d_r$. The constant component is set as $[5 \ 5]^T$ (m/s). Stochastic wind disturbance is modeled as follows [6]:

$$\dot{d}_r = \begin{bmatrix} \dot{d}_u \\ \dot{d}_v \end{bmatrix} = \begin{bmatrix} -1/\tau_c & 0 \\ 0 & -1/\tau_c \end{bmatrix} \begin{bmatrix} d_u \\ d_v \end{bmatrix} + \rho \begin{bmatrix} q_u \\ q_v \end{bmatrix},$$

where $\tau_c = 3.2$ s is the time constant; q_u and q_v ($\sigma_{q_u} = \sigma_{q_v} = 3.6576$ m/s) are independent with zero mean; $\rho = 1/2$. Figure 3 shows the wind disturbance d_w used in the helicopter’ simulation.

Additionally, the flapping dynamics model is considered to provide sufficient fidelity for the simulation process. Flapping dynamics are equivalent to the additional dynamics in the servo loop [28]:

$$\begin{aligned} \tau_f \dot{\delta}_{lon} &= -\tau_f q - \bar{\delta}_{lon} + \delta_{lon} \\ \tau_f \dot{\delta}_{lat} &= -\tau_f p - \bar{\delta}_{lat} + \delta_{lat}, \end{aligned} \tag{55}$$

where $\bar{\delta}_{lon}$ and $\bar{\delta}_{lat}$ are longitudinal and lateral applied control signals, respectively, and $\tau_f = 0.1$ is the main rotor’s dynamics time constant.

According to the flight characteristic of small-scale helicopters, the parameters of FT controller combined with DO (FT+DO) are selected properly, where $\tau = -2/31$, $\beta_1 = 2$, $\beta_2 = 5$, $\beta_3 = 20$, $\beta_4 = 50$, $\beta_{1\psi} = 20$, and $\beta_{2\psi} = 50$. The fourth-order SM DO is adopted, and the corresponding parameters are given as $L_1 = L_2 = 10$ and $L_3 = 20$.

To verify our controller’s superiority, the proposed controller is compared with BS and FT controller without DO. All the parameters of the FT controller are the same as that of FT+DO. BS controller has the following form

$$\begin{aligned} e_{P2d,bs} &= -k_{1,bs} e_{P1} \\ e_{P3d,bs} &= -k_{2,bs} (e_{P2} - e_{P2d,bs}) \end{aligned}$$

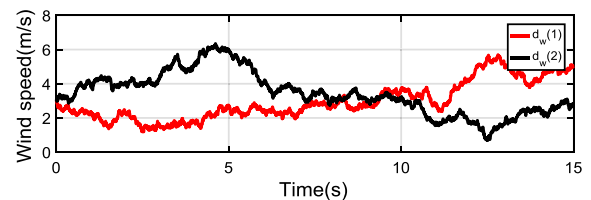


Fig. 3 Wind disturbance

Fig. 4 Trajectory tracking responses of the helicopter

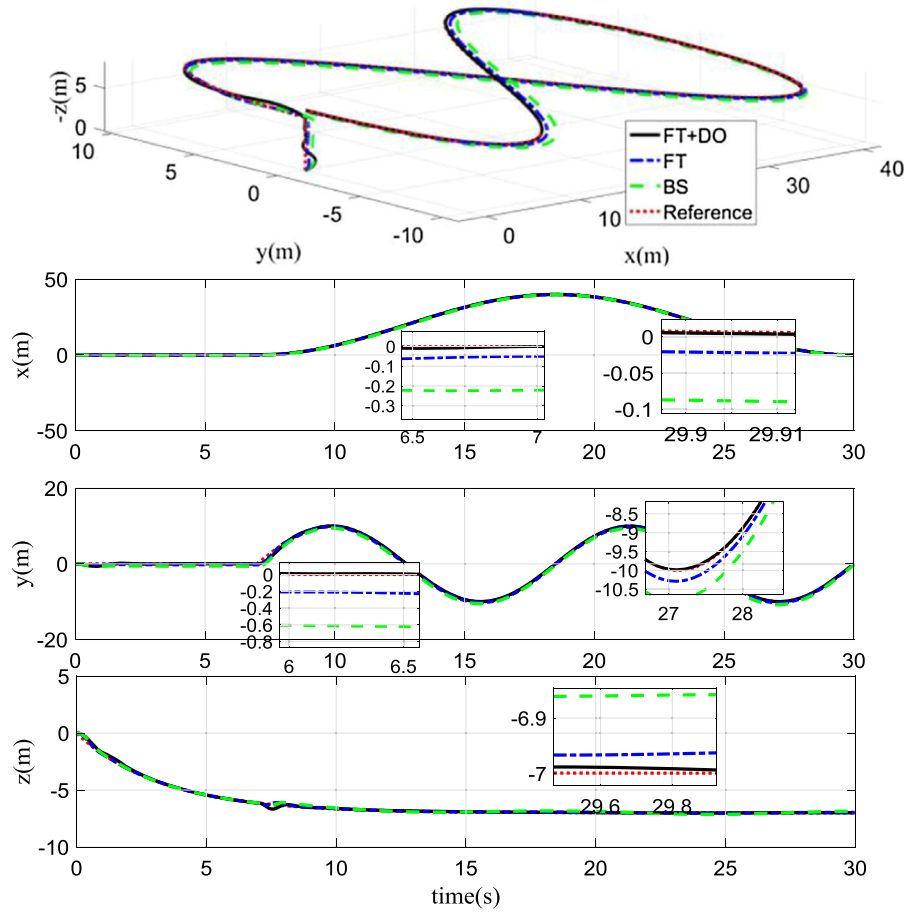


Fig. 5 Velocity response of the helicopter

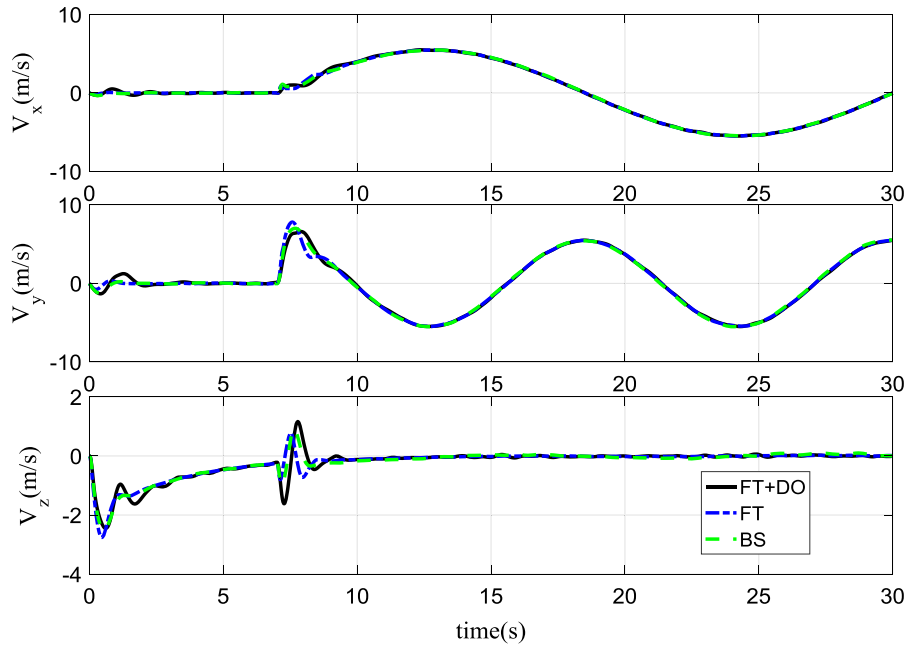


Fig. 6 Angular response of the helicopter

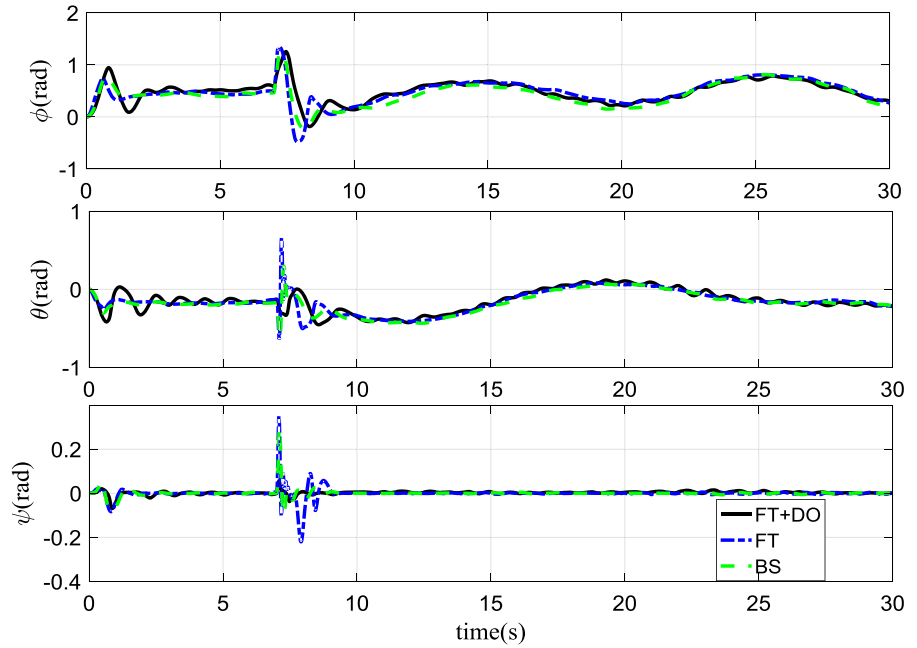
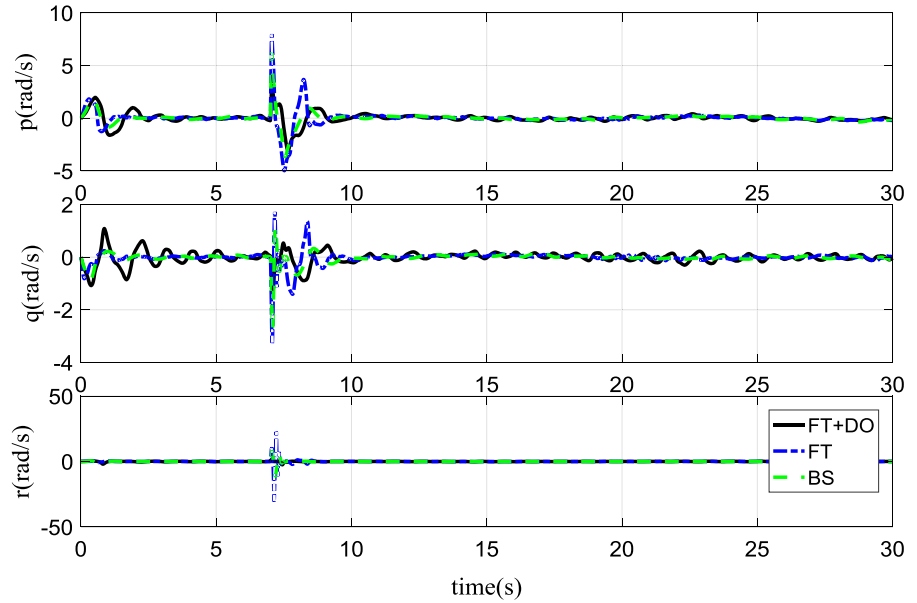


Fig. 7 Angular rate response of the helicopter



$$e_{p4d,bs} = -k_{3,bs} (e_{p3} - e_{p3d,bs})$$

$$u_p = -f_{pe}(t) - k_{4,bs} (e_{p4} - e_{p4d,bs})$$

$$e_{\psi 2d,bs} = -k_{1\psi,bs} e_{\psi 1}$$

$$u_\psi = -f_{\psi e}(t) - k_{2\psi,bs} (e_{\psi 2} - e_{\psi 2d,bs})$$

where $k_{1,bs} = 2$, $k_{2,bs} = 5$, $k_{3,bs} = k_{1\psi,bs} = 20$, and $k_{4,bs} = k_{2\psi,bs} = 50$. The comparison of BS controller highlights the benefits of FT method, which pro-

vides rapid convergent speed and improved disturbance rejection performance.

The desired “8-shape” reference trajectory is described as:

$$P_d(t) = \begin{cases} [0 \ 0 \ -7(1 - e^{-0.3t})]^T & \text{for } t \leq 7s \\ \begin{bmatrix} 20(1 - \cos(\frac{2\pi}{23}(t-7))) \\ 10 \sin(\frac{4\pi}{23}(t-7)) \\ -7(1 - e^{-0.3t}) \end{bmatrix} & \text{for } t > 7s \end{cases}$$

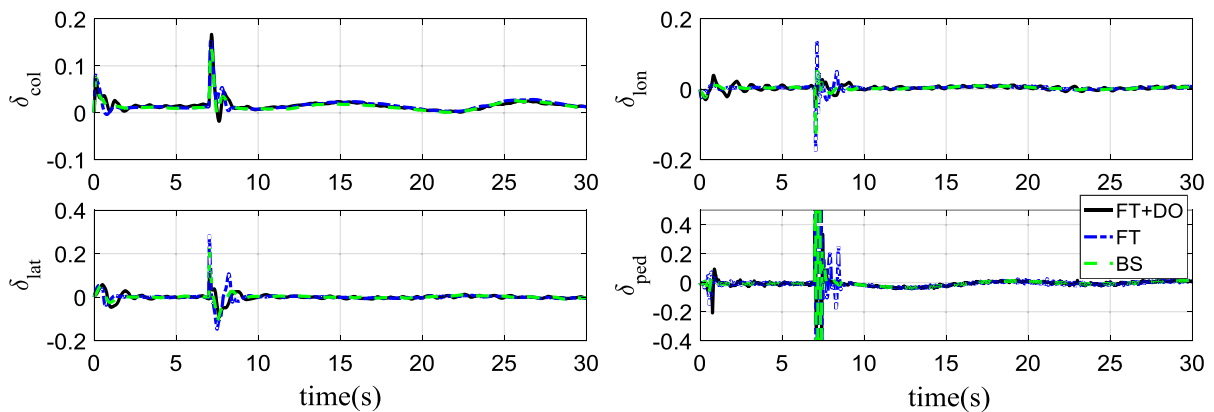


Fig. 8 Control commands of the helicopter

$$\psi_d = 0 \quad (56)$$

Firstly, the helicopter vertically climbs for 7 s to simulate the takeoff stage. Then, it follows an “8-shaped” path while continuing to lift. Helicopter’s lift, sideslip, and forward performances are evaluated comprehensively through the moderately aggressive maneuver.

The simulation results are illustrated in Figs. 4, 5, 6, 7, and 8. Figure 4 gives the position response curves of helicopter’s closed-loop system based on the three methods. To quantitatively analyze the tracking performance, the integrated time absolute error (ITAE defined as $\int_0^t t \|e\| dt$) of three methods is listed in Table 2. Our proposed FT+DO controller tracks the reference trajectory more accurately under model uncertainties and external disturbances than other controllers. Moreover, the comparison of BS and FT control shows that FT stability property not only enjoys convergence speed but also improves robustness of the closed-loop system. Figure 4 also gives the 3D position trajectory intuitively, and the results agree with this analysis. DO plays a significantly important role in the tracking accuracy of the closed-loop system. It attenuates the effect of perturbations and recure nominal performance of the control system.

The velocity, angle, and angular rate responses are shown in Figs. 5, 6, and 7. The state responses are a little chattering due to the existence of perturbations and fast tracking the maneuver trajectory. The responses of FT+DO fluctuate heavily to eliminate disturbances rapidly. Violent chattering exists at $t = 7$ s due to the switching of reference trajectory. Additionally, Fig. 8 displays the curves of controller commands. One can

Table 2 Average error of position tracking

Axis	X (m)	Y (m)	Z (m)
FT+DO	0.0186	0.0724	0.0104
FT	0.0301	0.1093	0.0165
BS	0.1009	0.2642	0.0379

find that the control signals of FT+DO method have smaller vibration than the other at the time of switching of the desired trajectory.

5 Conclusion

We design a composite FT control law for helicopter. The helicopter dynamics are simplified and decoupled by approximate feedback linearization. ADRC technique is utilized to realize the accurate trajectory tracking under matched and mismatched disturbances. The disturbances are estimated by HOSMDO and then feed-forwardly compensated for. The FT feedback part is designed via added power integrator method. The compound control law guarantees FT convergence of the tracking errors. Numerical simulation demonstrates that with this obtained FT controller in our work, a small-scale unmanned helicopter exhibits excellent tracking performance with disturbances.

Acknowledgements Funding was provided by National Natural Science Foundation of China (Grant No. U1613225)

Compliance with ethical standards

Conflict of interest None.

Appendix

Proof of Theorem 3

The proving course of finite-time (FT) stability is divided into two stages. First, FT stability is established when $t > t_{\max}$. Second, the states of the whole system are proven to not escape in any FT interval.

a) According to (41) and (49), $\dot{V}_4 + \dot{V}_{2\psi} \leq -\beta_{\max} \left[\sum_{i=1}^3 \left(e_{P1,i}^2 + (\xi_{2,i})^2 + (\xi_{3,i})^2 + (\xi_{4,i})^2 \right) + e_{\psi 1}^2 + (\xi_{2\psi})^2 \right] \leq 0$

where $\beta_{\max} = \max \{ \tilde{\beta}_1 \tilde{\beta}_2 \tilde{\beta}_3 \tilde{\beta}_4 \tilde{\beta}_{1\psi} \tilde{\beta}_{2\psi} \}$. In addition, considering the definition of the Lyapunov function, constant $L > 0$ exists such that

$$0 \leq V_4 + V_{2\psi} \leq L \left[\sum_{i=1}^3 \left(e_{P1,i}^{2-\tau} + (\xi_{2,i})^{2-\tau} + (\xi_{3,i})^{2-\tau} + (\xi_{4,i})^{2-\tau} \right) + e_{\psi 1}^{2-\tau} + (\xi_{2\psi})^{2-\tau} \right]$$

Select $\lambda = \beta_{\max}/2L^{2-\tau}$. The use of Lemma 3 produces

$$\begin{aligned} (V_4 + V_{2\psi})' + \lambda (V_4 + V_{2\psi})^{\frac{2}{2-\tau}} &\leq -\beta_{\max} \left[\sum_{i=1}^3 \left(e_{P1,i}^2 + (\xi_{2,i})^2 + (\xi_{3,i})^2 + (\xi_{4,i})^2 \right) + e_{\psi 1}^2 + (\xi_{2\psi})^2 \right] \\ &+ \lambda L^{\frac{2}{2-\tau}} \left[\sum_{i=1}^3 \left(e_{P1,i}^2 + (\xi_{2,i})^2 + (\xi_{3,i})^2 + (\xi_{4,i})^2 \right) + e_{\psi 1}^2 + (\xi_{2\psi})^2 \right] \\ &\leq 0 \end{aligned}$$

By applying Theorem 1, we conclude that the state vector will converge on zero in FT.

b) In this step, proof that the helicopter’s state does not escape to infinite in any FT interval is provided. Combining simplified helicopter dynamic system (18), DO (20), and controllers (40) and (48), the following closed-loop dynamics are introduced

$$\begin{aligned} \dot{e}_{P1} &= e_{P2} \\ \dot{\xi}_{2,i} &= \frac{1}{r_2} (e_{P2,i})^{\frac{1}{r_2}-1} (\bar{e}_{P3,i} - \sigma_{1,1,i}) + (\beta_1)^{\frac{1}{r_2}} e_{P2,i} \\ \dot{\xi}_{3,i} &= \frac{1}{r_3} (\bar{e}_{P3,i})^{\frac{1}{r_3}-1} (\bar{e}_{P4,i} - \sigma_{2,1,i}) + (\beta_2)^{\frac{1}{r_3}} \dot{\xi}_2 \end{aligned}$$

$$\begin{aligned} \dot{\xi}_{4,i} &= \frac{1}{r_4} (\bar{e}_{P4,i})^{\frac{1}{r_4}-1} (-\beta_4 (\xi_{4,i})^{r_5} - \sigma_{3,1,i} - \sigma_{1,2,i}) \\ &+ (\beta_3)^{\frac{1}{r_4}} \dot{\xi}_3 \end{aligned}$$

$$\begin{aligned} \dot{e}_{\psi 1} &= e_{\psi 2} \\ \dot{\xi}_{2\psi} &= \frac{1}{r_2} (e_{\psi 2})^{\frac{1}{r_2}-1} (-\beta_{2\psi} (\xi_{2\psi})^{r_3} - \sigma_{3,1}) \\ &+ (\beta_1)^{\frac{1}{r_2}} e_{\psi 2} \end{aligned} \tag{a1}$$

A Lyapunov function is selected as follows:

$$\begin{aligned} L &= \frac{1}{2} \sum_{i=1}^3 \left[(e_{P1})^2 + (\xi_{2,i})^2 + (\xi_{3,i})^2 + (\xi_{4,i})^2 \right] \\ &+ \frac{1}{2} \left[(e_{\psi 1})^2 + (\xi_{2\psi})^2 \right] \end{aligned} \tag{a2}$$

Its derivative is expressed as follows:

$$\begin{aligned} \dot{L} &= e_{P1} \dot{e}_{P1} + \xi_2 \dot{\xi}_2 + \xi_3 \dot{\xi}_3 + \xi_4 \dot{\xi}_4 \\ &= \sum_{i=1}^3 [e_{P1,i} e_{P2,i}] \\ &+ \sum_{i=1}^3 \left[\xi_{2,i} \left(\frac{1}{r_2} (e_{P2,i})^{\frac{1}{r_2}-1} (\bar{e}_{P3,i} - \sigma_{1,1,i}) + (\beta_1)^{\frac{1}{r_2}} e_{P2,i} \right) \right] \\ &+ \sum_{i=1}^3 \left[\xi_{3,i} \left(\frac{1}{r_3} (\bar{e}_{P3,i})^{\frac{1}{r_3}-1} (\bar{e}_{P4,i} - \sigma_{2,1,i}) + (\beta_2)^{\frac{1}{r_3}} \dot{\xi}_2 \right) \right] \\ &+ \sum_{i=1}^3 \left[\xi_{4,i} \left(\frac{1}{r_4} (\bar{e}_{P4,i})^{\frac{1}{r_4}-1} (-\beta_4 (\xi_{4,i})^{r_5} - \sigma_{3,1,i} - \sigma_{1,2,i}) + (\beta_3)^{\frac{1}{r_4}} (\dot{\xi}_3) \right) \right] \\ &+ e_{\psi 2} e_{\psi 1} + \xi_{2\psi} \left(\frac{1}{r_2} (e_{\psi 2})^{\frac{1}{r_2}-1} (-\beta_{2\psi} (\xi_{2\psi})^{r_3} - \sigma_{3,1}) + (\beta_1)^{\frac{1}{r_2}} e_{\psi 2} \right) \end{aligned}$$

To simplify the analysis, the following inequalities are obtained using Lemmas 1–2.

$$\begin{aligned} e_{P1,i} e_{P2,i} &\leq e_{P1,i} \left(|e_{P2,i} - e_{P2,i}^*| + |\beta_1 e_{P1,i}^{r_2}| \right) \\ &\leq |e_{P1,i}|^{2+\tau} + l_1 |\xi_{2,i}|^{2+\tau} \\ \xi_{2,i} \left(\frac{1}{r_2} (e_{P2,i})^{\frac{1}{r_2}-1} (\bar{e}_{P3,i} - \sigma_{1,1,i}) \right) &\leq \frac{1}{r_2} \xi_{2,i} \left(|e_{P2,i} - e_{P2,i}^*| + |\beta_1 e_{P1,i}^{r_2}| \right)^{\frac{1}{r_2}-1} \end{aligned}$$

$$\begin{aligned} & (|e_{P3,i} - e_{P3,i}^*| + |\beta_2 (\xi_{2,i})^{r_3}| - \sigma_{1,1,i}) \\ & \leq |e_{P1,i}|^{2+\tau} + l_{21} |\xi_{2,i}|^{2+\tau} + l_{22} |\xi_{3,i}|^{2+\tau} \\ & \quad + l_{23} |\sigma_{1,1,i}| (|e_{P1,i}|^{2-r_2} + |\xi_{2,i}|^{2-r_2}) \\ & \xi_{2,i} (\beta_1)^{\frac{1}{r_2}} e_{P2,i} \leq l_{24} |e_{P1,i}|^{2+\tau} + l_{25} |\xi_{2,i}|^{2+\tau} \end{aligned}$$

Similarly,

$$\begin{aligned} & \xi_{3,i} \left(\frac{1}{r_3} (\bar{e}_{P3,i})^{\frac{1}{r_3}-1} (\bar{e}_{P4,i} - \sigma_{2,1,i}) + (\beta_2)^{\frac{1}{r_3}} \dot{\xi}_2 \right) \\ & \leq \xi_{3,i} \left(\frac{1}{r_3} (|e_{P3,i} - e_{P3,i}^*| + |\beta_2 (\xi_{2,i})^{r_3}|)^{\frac{1}{r_3}-1} \right. \\ & \quad \left. (\bar{e}_{P4,i} - \sigma_{2,1,i}) + (\beta_2)^{\frac{1}{r_3}} \dot{\xi}_2 \right) \\ & \leq |e_{P1,i}|^{2+\tau} + l_{31} |\xi_{2,i}|^{2+\tau} + l_{32} |\xi_{3,i}|^{2+\tau} \\ & \quad + l_{33} |\xi_{3,i}|^{2+\tau} + l_{34} |\xi_{4,i}|^{2+\tau} \\ & \quad + l_{35} |\sigma_{2,1,i}| (|\xi_{2,i}|^{2-r_3} + |\xi_{3,i}|^{2-r_3}) \\ & \quad + l_{36} |\sigma_{1,1,i}| (|e_{P1,i}|^{2-r_2} + |\xi_{2,i}|^{2-r_2} + |\xi_{3,i}|^{2-r_2}) \\ & \xi_{4,i} \left(\frac{1}{r_4} (\bar{e}_{P4,i})^{\frac{1}{r_4}-1} (-\beta_4 (\xi_{4,i})^{r_5} - \sigma_{3,1,i} - \sigma_{1,2,i}) \right. \\ & \quad \left. + (\beta_3)^{\frac{1}{r_4}} (\dot{\xi}_3) \right) \\ & \leq |e_{P1,i}|^{2+\tau} + l_{41} |\xi_{2,i}|^{2+\tau} + l_{42} |\xi_{3,i}|^{2+\tau} \\ & \quad + l_{43} |\xi_{3,i}|^{2+\tau} + l_{44} |\xi_{4,i}|^{2+\tau} \\ & \quad + l_{45} |\sigma_{2,1,i} + \sigma_{1,2,i}| (|\xi_{3,i}|^{2-r_4} + |\xi_{4,i}|^{2-r_4}) \\ & \quad + l_{46} |\sigma_{2,1,i}| (|\xi_{2,i}|^{2-r_3} + |\xi_{3,i}|^{2-r_3} + |\xi_{4,i}|^{2+\tau}) \\ & \quad + l_{47} |\sigma_{1,1,i}| (|e_{P1,i}|^{2-r_2} + |\xi_{2,i}|^{2-r_2} \\ & \quad + |\xi_{3,i}|^{2-r_2} + |\xi_{4,i}|^{2-r_2}) \\ & e_{\psi 2} e_{\psi 2} + \xi_{2\psi} \left(\frac{1}{r_2} (e_{\psi 2})^{\frac{1}{r_2}-1} (-\beta_{2\psi} (\xi_{2\psi})^{r_3} - \sigma_{3,1}) \right. \\ & \quad \left. + (\beta_1)^{\frac{1}{r_2}} e_{\psi 2} \right) \\ & \leq l_{1\psi} |e_{\psi 2}|^{2+\tau} + l_{2\psi} |\xi_{2\psi}|^{2+\tau} + l_{3\psi} |\sigma_{1,3}| \\ & \quad (|e_{\psi 2}|^{2-r_2} + |\xi_{2\psi}|^{2-r_2}) \end{aligned}$$

where $l_{i,j} > 0$ is the bounded constant.

The control loop has no effects on the DO loop. When $t > t_{\max}$, the estimation errors of disturbances converge to zero. Therefore, the errors $\sigma_{i,j}$ are bounded. If $\max\{|e_{P1,i}|, |\xi_{2,i}|, |\xi_{3,i}|, |\xi_{4,i}|,$

$|e_{\psi 2}|, |\xi_{2\psi}|\} \leq 1$, then $\dot{L} \leq B$, where B is a bounded constant. If $\max\{|e_{P1,i}|, |\xi_{2,i}|, |\xi_{3,i}|, |\xi_{4,i}|, |e_{\psi 2}|, |\xi_{2\psi}|\} > 1$ because $2 + \tau < 2$ and $2 - r_2 < 2$, then $\dot{L} \leq KL + B$, where K is a bounded constant. Thus, $\dot{L} \leq KL + B$. (a3)

Reference [29] proves that the system state in (a2) will not escape to infinite in any FT.

According to the two stages of analysis, the proof of the FT stability is completed. \square

References

1. Mettler, B.: Identification Modeling and Characteristics of Miniature Rotorcraft. Kluwer Academic Publishers, Boston (2003)
2. Kendoul, F.: Survey of advances in guidance, navigation, and control of unmanned rotorcraft systems. *J. Field Robot.* **29**(2), 315–378 (2012)
3. Alvarenga, J., Vitzilaios, N.I., Valavanis, K.P., Rutherford, M.J.: Survey of unmanned helicopter model-based navigation and control techniques. *J. Intell. Robot. Syst.* **80**(1), 87–138 (2015)
4. Cai, G.W., Chen, B.M., Lee, T.H.: Unmanned Rotorcraft Systems. Springer, Heidelberg (2011)
5. Tanner, O.: Modeling, Identification, and Control of Autonomous Helicopters. Ph. D thesis, ETH (2003)
6. Gadewadikar, J., Chen, B.M., Subbarao, K.: Structured H_∞ command and control-loop design for unmanned helicopters. *J. Guid. Control Dyn.* **31**(4), 1093–1102 (2008)
7. Civita, M.L., Papageorgiou, G., Messner, W.C., Kanade, T.: Design and flight testing of a gain-scheduled H_∞ loop shaping controller for wide-envelope flight of a robotic helicopter. In: Proceedings of American Control Conference, Denver, USA, pp. 4195–4200 (2003)
8. Raptis, I.A., Valavanis, K.P., Moreno, W.A.: A novel nonlinear backstepping controller design for helicopters using the rotation matrix. *IEEE Trans. Control Syst. Technol.* **19**(2), 465–473 (2011)
9. Zhu, B., Huo, W.: Robust nonlinear control for a model-scaled helicopter with parameter uncertainties. *Nonlinear Dyn.* **73**(1–2), 1139–1154 (2013)
10. He, Y.B., Pei, H.L., Sun, T.R.: Robust tracking control of helicopters using backstepping with disturbance observers. *Asian J. Control* **16**(6), 1–16 (2014)
11. Aboudonia, A., El-Badawy, A., Rashad, R.: Active anti-disturbance control of a quadrotor unmanned aerial vehicle using the command-filtering backstepping approach. *Nonlinear Dyn.* **90**(1), 581–597 (2017)
12. Shao, X.L., Liu, J., Cao, H.L., Shen, C., Wang, H.L.: Robust dynamic surface trajectory tracking control for a quadrotor UAV via extended state observer. *Int. J. Robust Nonlinear Control* **28**(7), 2700–2719 (2018)
13. Simplicio, P., Pavel, M.D., Kampen, E.V., Chu, Q.P.: An acceleration measurements-based approach for helicopter nonlinear flight control using Incremental Nonlinear Dynamic Inversion. *Control Eng. Pract.* **21**(9), 1065–1077 (2013)

14. Xing, F., Wu, A.G., Shang, Y.J., Dong, N.: A novel sliding mode controller for small-scale unmanned helicopters with mismatched disturbance. *Nonlinear Dyn.* **83**(1–2), 1053–1068 (2016)
15. Liu, C.J., Chen, W.H., Andrews, H.: Tracking control of small-scale helicopters using explicit nonlinear MPC augmented with disturbance observers. *Control Eng. Pract.* **20**(3), 258–268 (2012)
16. Isidori, A., Marconi, L., Serrani, A.: Robust nonlinear motion control of a helicopter. *IEEE Trans. Autom. Control* **48**(3), 413–426 (2003)
17. Huang, Y., Xue, W.C.: Active disturbance rejection control: methodology and theoretical analysis. *ISA Trans.* **53**, 963–976 (2014)
18. Chen, W.H., Yang, J., Guo, L., Li, S.H.: Disturbance-observer-based control and related methods—an overview. *IEEE Trans. Ind. Electron.* **63**(2), 1083–1095 (2016)
19. Bhat, S.P., Bernstein, D.S.: Continuous finite-time stabilization of the translational and rotational double integrators. *IEEE Trans. Autom. Control* **43**(5), 678–682 (1998)
20. Bhat, S.P., Bernstein, D.S.: Finite-time stability of continuous autonomous systems. *SIAM J. Control Optim.* **38**(3), 751–766 (2000)
21. Qian, C.J., Wei, L.: A continuous feedback approach to global strong stabilization of nonlinear systems. *IEEE Trans. Autom. Control* **46**(7), 1061–1079 (2001)
22. Huang, X.Q., Wei, L., Yang, B.: Global finite-time stabilization of a class of uncertain nonlinear systems. *Automatica* **41**, 881–888 (2005)
23. Polendo, J., Qian, C.J.: An expanded method to robustly stabilize uncertain nonlinear systems. *Commun. Inf. Syst.* **6**(1), 55–70 (2008)
24. Levant, A.: Higher-order sliding modes, differentiation and output-feedback control. *Int. J. Control* **76**(9), 924–941 (2003)
25. Li, S.H., Sun, H.B., Yang, J., Yu, X.H.: Continuous finite-time output regulation for disturbed systems under mismatching condition. *IEEE Trans. Autom. Control* **1**(60), 277–282 (2015)
26. Sun, H.B., Hou, L.L., Zong, G.D.: Continuous finite time control for static var compensator with mismatched disturbances. *Nonlinear Dyn.* **85**, 2159–2169 (2016)
27. Koo, T.J., Sastry, S.: Output tracking control design of a helicopter model based on approximate linearization. In: *Proceedings of 37th IEEE Decision and Control*, Tampa, USA, pp. 3635–3640 (1998)
28. Gavrillets, V.: *Autonomous Aerobatic Maneuvering of Miniature Helicopters*. Ph. D thesis, MIT (2003)
29. Khalil, H.K.: *Nonlinear Systems*, 3rd edn. Prentice Hall, Upper Saddle River, NJ (2002)

Publisher's Note Springer Nature remains neutral with regard to jurisdictional claims in published maps and institutional affiliations.